Inflammation-Generated Extracellular Matrix Fragments Drive Lung Metastasis

Sandrine Bekaert[1], Marianne Fillet[2,3], Benoit Detry[1], Muriel Pichavant[4], Raphael Marée[5], Agnes Noel[1], Natacha Rocks[1*] and Didier Cataldo[1*]

[1]Laboratory of Tumor and Development Biology, GIGA-Research (Groupe Interdisciplinaire de Génoprotéomique Appliquée-Recherche)—GIGA-Cancer, University of Liège and CHU of Liège, Liège, Belgium. [2]Laboratory of Analytical Pharmaceutical Chemistry, Department of Pharmacy, CIRM, University of Liège, Liège, Belgium. [3]Laboratory of Clinical Chemistry, GIGA-Research, University of Liège, Liège, Belgium. [4]Institut Pasteur de Lille, Centre d'Infection et d'Immunité de Lille, Lille, France. [5]GIGA Bioinformatics Platform, University of Liège, Liège, Belgium.

ABSTRACT: Mechanisms explaining the propensity of a primary tumor to metastasize to a specific site still need to be unveiled, and clinical studies support a link between chronic inflammation and cancer dissemination to specific tissues. Using different mouse models, we demonstrate the role of inflammation-generated extracellular matrix fragments ac-PGP (*N*-acetyl-proline-glycine-proline) on tumor cells dissemination to lung parenchyma. In mice exposed to cigarette smoke or lipopolysaccharide, lung neutrophilic inflammation produces increased levels of MMP-9 (matrix metalloproteinase 9) that contributes to collagen breakdown and allows the release of ac-PGP tripeptides. By silencing CXCR2 gene expression in tumor cells, we show that these generated ac-PGP tripeptides exert a chemotactic activity on tumor cells in vivo by binding CXCR2.

KEYWORDS: lung metastasis, microenvironment, neutrophilic inflammation, MMP-9, ac-PGP, matrikine, CXCR2

Introduction

About 90% of cancer-related deaths are attributable to the metastatic spread of the primary tumor.[1] The importance of the relationship between microenvironment and tumor cells has become evident. However, precise mechanisms for the propensity of primary tumors to metastasize to a specific site are still to be unveiled. Tissues are in many circumstances (eg, exposure to cigarette smoke [CS], pollution, or infectious agents) infiltrated by immune cells and contain cytokines, chemokines, and growth factors that might significantly contribute to the seeding of metastatic cancer cells.[2,3] Epidemiologic studies repetitively reported that many human cancers in adults are associated with chronic inflammation in different organs.[4,5] Moreover, it is now clearly established that neutrophils can modulate immune responses within tumor microenvironment and interfere with tumor development in different manners (eg, establish a permissive microenvironment that favors tumor growth).[6] In humans, chronic obstructive pulmonary disease (COPD)-related inflammatory processes in smokers are associated with an increased risk of lung cancer as compared with smokers who do not have COPD.[7] In these patients, tobacco smoke exposure induces a rapid recruitment of neutrophils to lung tissues through a gradient of ELR+ ("glu-leu-arg" motif) CXC chemokine such as CXCL8.[8,9]

The mechanisms that might explain the favoring effect of neutrophils on cancer progression are still debated and it is established that these cells display immunomodulatory properties.[10] Hence, neutrophil-derived mediators released in lung microenvironment such as leukotrienes strongly support lung metastasis dissemination from breast cancer cells.[11] Neutrophils are able to interact with cells and extracellular matrix and the release of proteases as matrix metalloproteinase 9 (MMP-9) or other cytotoxic mediators can cause tissue damage in many diseases. MMP-9 plays important roles in tissue destruction and inflammation through proteolytic cleavages resulting in degradation of matrix proteins and activation of cytokines/chemokines. It was previously shown that collagen breakdown by MMP-8 and MMP-9 followed by a prolyl endopeptidase cleavage generates *N*-acetyl-proline-glycine-proline (ac-PGP) tripeptides.[12–16]

The ac-PGP tripeptides have been reported to bind CXCR2 and trigger chemotaxis of inflammatory cells.[17–19] In non–small-cell lung cancer samples, CXCR2 expression has been correlated with tumor inflammation and angiogenesis[20] and has been associated with a poorer prognosis.[21] Furthermore, in malignant breast cancer tissues, CXCR2 signaling plays a key role in tumor cell invasion and metastatic dissemination to lung tissues.[22] Interestingly, ac-PGP was also detected in the bronchoalveolar lavage (BAL), sputum, and serum from patients with COPD.[23] The molecular basis for ac-PGP chemoattractant effects on

---

*N.R. and D.C. contributed equally to this work.

neutrophils relies on ac-PGP structural homology with the "GP" motif shared by all ELR+ CXC chemokines, including CXCL8.[24] Moreover, CXCR2 is expressed not only by neutrophils but also by a large variety of tumor cells originating from lung, melanoma, pancreatic, ovarian, and breast tissues, suggesting a possible role for ac-PGP tripeptides in tumor cell chemoattraction.[21]

In this study, we explored the impact of extracellular matrix fragments (ac-PGP) generated by a pulmonary inflammatory burden induced by CS or lipopolysaccharide (LPS) instillation on cancer cell dissemination to lung parenchyma. MMP-9 originating from neutrophils generated collagen breakdown and the production of chemotactic ac-PGP that attracts tumor cells to lung parenchyma. The role of ac-PGP in cancer cells dissemination to lung was confirmed by synthetic ac-PGP instillation into the lungs. By silencing CXCR2 on tumor cells, we also demonstrate that the chemotactic effect of ac-PGP on tumor cells is dependent on CXCR2.

Materials and Methods

Cell culture

Murine melanoma B16F10 and murine mammary cancer 4T1 cell lines were purchased from Caliper Life Sciences (Hopkinton, MA, USA). Murine melanoma B16F10 cells were grown in RPMI-1640 (Roswell Park Memorial Institute; Lonza, Basel, Switzerland) supplemented with 10% fetal bovine serum (FBS) and 2 mmol/L L-glutamine, penicillin-streptomycin (100 IU/mL-100 µg/mL) (Life Technologies, Carlsbad, CA, USA). 4T1 cells, stably transfected with the luciferase gene, and 4T1-shCXCR2 cells were cultured in Dulbecco's Modified Eagle Medium (Life Technologies) supplemented with 10% FBS and 2 mmol/L L-glutamine, penicillin-streptomycin (100 IU/mL-100 µg/mL) (Life Technologies). Silencing of CXCR2 gene expression achieved using short hairpin RNA (shRNA) technology is described in supplemental experimental procedures.

Mice

Male C57Bl/6J and BALB/c mice, 6 to 8 weeks old, weight ±20 g, were purchased from Charles River (Cologne, Germany). MMP-9 knockout (MMP-9$^{-/-}$) mice and the corresponding wild-type (MMP-9$^{+/+}$) mice were originally obtained from the Department of Anatomy, University of California, San Francisco (Z. Werb, UCSF)[25] and bred in our facility. All animal experimental procedures were approved by the ethical committee of the University of Liège.

Metastasis assays

Metastatic dissemination of murine melanoma B16F10 cells, murine mammary cancer 4T1 cells, and 4T1-shCXCR2 cells to lung tissues was investigated using 2 distinct metastasis models in syngeneic mice after inducing a pulmonary inflammation by CS or LPS exposure or ac-PGP/*N*-acetyl valine-alanine-valine (ac-VAV) stimulation.

Intravenous model—Mainstream CS exposure. C57Bl/6 mice (n = 8/group) were exposed to whole-body mainstream CS during 5 days per week and up to 5 weeks. For this, mice were placed in an inhalation chamber and daily exposed to 5 cigarettes with filters (Kentucky reference 3R4F; University of Kentucky Tobacco and Health Research Institute, Lexington, KY, USA). The negative-control group was exposed to ambient air. After 2 weeks of the start of CS exposure, murine melanoma B16F10 cells (1 × 10^5 cells/50 µL in serum-free medium) were injected into the lateral tail vein of mice.

Intravenous model—LPS stimulation protocol. Mice (n = 8/group) were anesthetized with 2.5% isoflurane/oxygen mixture and intratracheally injected with phosphate-buffered saline (PBS) or LPS (3 µg/100 µL, ultrapure LPS from *Escherichia coli*, Invivo-Gen, San Diego, CA, USA), 3 times per week to maintain a stable level of inflammation in the lung parenchyma over time. After 4 LPS instillations, murine melanoma B16F10 cells or murine mammary cancer 4T1 cells (1 × 10^5 cells/50 µL in serum-free medium) were injected into the lateral tail vein of C57Bl/6 or Balb/c mice, respectively. MMP-9$^{+/+}$ and MMP-9$^{-/-}$ mice were injected with B16F10 cells (n = 6/group). Murine mammary cancer 4T1 cells were stably transfected with luciferase gene, which allowed a regular follow-up of pulmonary metastasis evolution. For noninvasive bioluminescence visualization of metastasis, Balb/c mice were injected intraperitoneally with D-luciferin (150 mg/kg in PBS; Promega, Madison, WI, USA) and anesthetized with 2.5% isoflurane-oxygen mixture. After 12 minutes of D-luciferin injection, mice were placed in IVIS 200 Imaging System (Caliper Life Sciences) and imaged for 1 minute. A quantitative assessment of metastasis was performed by determining "regions of interest" in the lungs and measuring bioluminescence intensity using Living Image software.

Subcutaneous cancer dissemination model—LPS stimulation protocol. Mice were instilled 3 times per week with PBS or LPS (3 µg/100 µL) (*vide supra*). After 4 LPS instillations, murine mammary cancer cells 4T1 (2 × 10^5 cells/100 µL in serum-free medium) were subcutaneously injected into flanks of mice (n = 8 mice/group). Lung metastasis was assessed by measuring bioluminescence in vivo using the IVIS 200 Imaging System.

Intravenous cancer dissemination model—Ac-PGP and ac-VAV stimulation protocol. Balb/c mice (n = 5/group) were anesthetized with 2.5% isoflurane/oxygen and intratracheally injected with PBS or ac-PGP (250 µg/200 µL; Eurogentec, Seraing, Belgium) or ac-VAV (250 µg/200 µL; Eurogentec), 3 times per week. After 4 ac-PGP or ac-VAV instillations, murine mammary cancer 4T1 cells or 4T1-shCXCR2 cells (1 × 10^5 cells/50 µL in serum-free medium) were injected into the lateral tail vein of Balb/c mice. Lung metastasis was assessed by measuring bioluminescence in vivo using the IVIS 200 Imaging System.

At the end of each experimental protocol, animals were sacrificed and a BAL was collected via intratracheal instillation of

4 mL × 1 mL PBS-EDTA 0.05 mM solution (Calbiochem, Darmstadt, Germany). Bronchoalveolar lavage fluid was collected for protein assessment, whereas cells were used for differential cell counts. Differential cell counts based on morphologic criteria were performed on cytocentrifuged preparations after staining with hematoxylin-eosin (Diff-Quick, Dade, Belgium).

Pulmonary histology and immunohistochemistry

Metastasis to lung tissues was evaluated by measuring tumor area in lungs and reporting it to the total area of lung tissues analyzed, on 8 hematoxylin-eosin–stained sections per animal using Cytomine software.[26] Proliferating and apoptotic cells were visualized on tumor sections using antibodies raised against Ki-67 and double-stranded DNA as described in supplemental experimental procedures.

Tissue processing and labeling of total cell lung suspension for flow cytometry

To identify mouse granulocyte subpopulations, digested lungs were stained with following antibodies: CD45, CCR3, CD11b, 7/4 antigen (Ly6B.2), GR1, CD11c, and CD3. More details about preparation of mouse lungs for inflammatory cells analysis by flow cytometry are described in the supplemental materials and methods section.

Tumor cell chemotaxis assay

Neutrophil supernatant (SN) preparation and tumor cell chemotaxis processing are detailed in the supplemental materials and methods section. After 48 hours of incubation in Transwell plates, migration of cells was evaluated by reporting area of cells present on the filter to the total filter area.

Lung extravasation assay

To evaluate short-term extravasation of tumor cells toward lungs of pretreated mice, Red CMTPX–stained 4T1 cells were injected intravenously. After 48 hours of cell injection, a lung perfusion was realized and extravasated tumor cells were counted by confocal microscopy. More details about this procedure are described in the supplemental materials and methods section.

Ac-PGP quantification in serum samples

To perform ac-PGP quantification, calibration curves were performed with ac-PGP standard solutions in the concentration range of 25 to 250 pg/mL. Internal standard, which consists of ac-PGP isotopically labeled with ^{13}C on proline, was added in all samples at the same concentration. Details of LC-Chip nano high-performance liquid chromatography electrospray MS-MS to analyze samples are explained in the supplemental materials and methods section.

Statistical analysis

Reported values are expressed as mean ± SEM. Statistical analysis differences between experimental groups were assessed using InStat software (GraphPad, La Jolla, CA, USA). Data were analyzed by the Student *t* test. Variations were considered to be statistically significant at *$P < .05$ or **$P < .01$.

Results

Chronic exposure to CS induces a neutrophilic pulmonary inflammation and increases lung metastasis of B16F10 melanoma cells

To analyze the effects of CS on metastatic dissemination of tumor cells, C57/Bl6 mice were exposed during 5 weeks to CS or air and intravenously injected with melanoma B16F10 cells. In mice exposed to CS, a drastic increase in melanoma cell retention in lung tissue was observed (Figure 1A). Lung area occupied by tumor cells was 3-fold higher in CS-exposed mice as compared with air-exposed mice (n = 8/experimental condition; **$P < .01$; Figure 1B). To verify whether this increased melanoma cell detection in CS-challenged lung tissues could be attributed to a change in tumor cell proliferation or apoptosis, an anti-Ki67 immunohistochemistry was performed on lung tissue slides and showed that tumor cell proliferation in metastatic foci was slightly reduced by CS exposure (data not shown), indicating that tobacco smoke does not directly induce tumor cell proliferation in vivo. Likewise, a TUNEL (terminal deoxynucleotidyl transferase dUTP nick end labeling) assay performed on lung tissue sections did not reveal any difference in apoptosis rates of tumor cells between CS and air-treated mice.

To analyze the effects of CS on the recruitment of inflammatory cells, a BAL was performed after mice were exposed to CS during 5 weeks and showed increased neutrophil percentages in CS-exposed mice injected with B16F10 cells (2.82% ± 0.94% in control group versus 5.90% ± 1.18% in CS group) or not injected with tumor cells (1.33% ± 0.33% in control group versus 5% ± 2.21% in CS group). This CS-induced neutrophil influx was also measured by flow cytometry performed on digested lungs after 2 weeks of CS exposure. An increased proportion of GR1+ Ly6b+ population identified as neutrophils (P4) was detected in lung lysates of CS-exposed mice (34.35%) as compared with control mice (16.6%) (Figure 1C).

Neutrophils promote cancer cell migration and extravasation

To investigate whether the environment-induced neutrophilic inflammation triggers organ colonization by metastasis, C57Bl/6 mice were treated with a pulmonary, acute neutrophil-inducing stimulus (LPS). Mice were pretreated by intratracheal instillations of PBS or LPS and intravenously injected with B16F10 cells. Mice stimulated with LPS displayed increased BAL neutrophil percentages (n = 8 per group, 1.37% ± 1.05% and 1.93% ± 0.67% in control (PBS) and
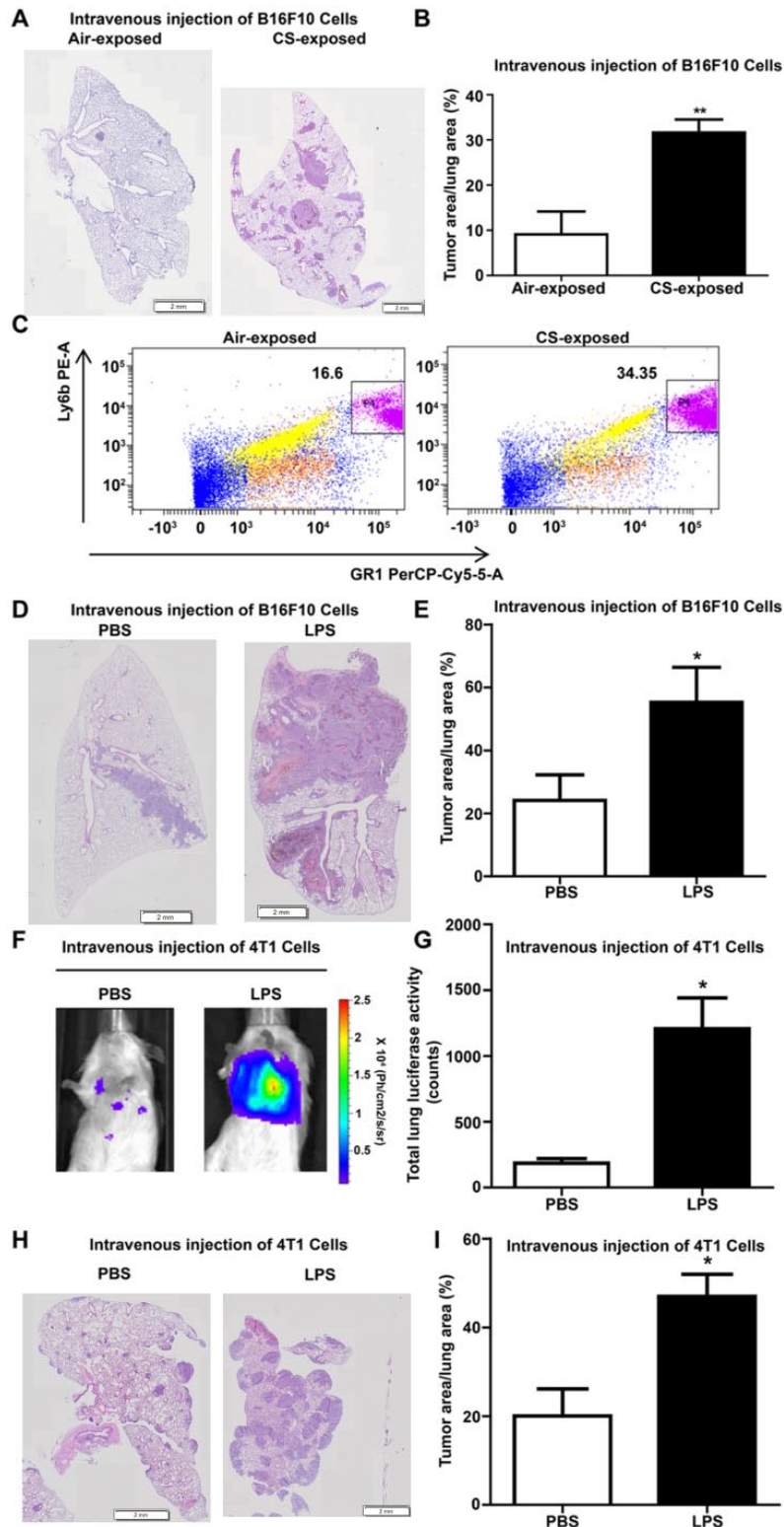
Figure 1. Neutrophil inflammation induces tumor cell dissemination to lung tissue. (A) Representative hematoxylin-eosin–stained sections of lung tissues (5 weeks of cigarette smoke [CS] or ambient air [air] exposure, intravenous B16F10 melanoma cell injection 2 weeks after test begins), n = 8 (hematoxylin-eosin). (C) Percentages of neutrophils in lung lysates from mice exposed to Air or CS during 2 weeks. Selected windows identify Ly6b+ GR1+ neutrophils. Results are expressed as percentage of positive cells. (D) Representative hematoxylin-eosin–stained sections of lung tissues 2 weeks after intravenous injection of B16F10 melanoma cells and pulmonary challenge with PBS or LPS, n = 8 (hematoxylin-eosin). (F) Biophotonic monitoring of lung metastasis in animals intravenously injected with luciferase-transfected 4T1 cells and treated with intratracheal injections of PBS or LPS. (G) Quantification of bioluminescence in regions of interest (ROI) determined around lungs. (H) Representative hematoxylin-eosin–stained sections of lung tissues 2 weeks after intravenous 4T1 cell injection and intratracheal stimulation with PBS or LPS, n = 8 (hematoxylin-eosin). (B, E, I) Tumor size quantification was assessed by measuring the ratio between the area of tumor foci in lungs and total lung tissue area on 8 sections per mouse in each group. Results are expressed as mean tumor area/lung area ± SEM and are representative of 2 individual experiments. **$P < .01$; *$P < .05$. Scale bar: (A, D) 2 mm, (H) 1 mm. LPS indicates lipopolysaccharide; PBS, phosphate-buffered saline.
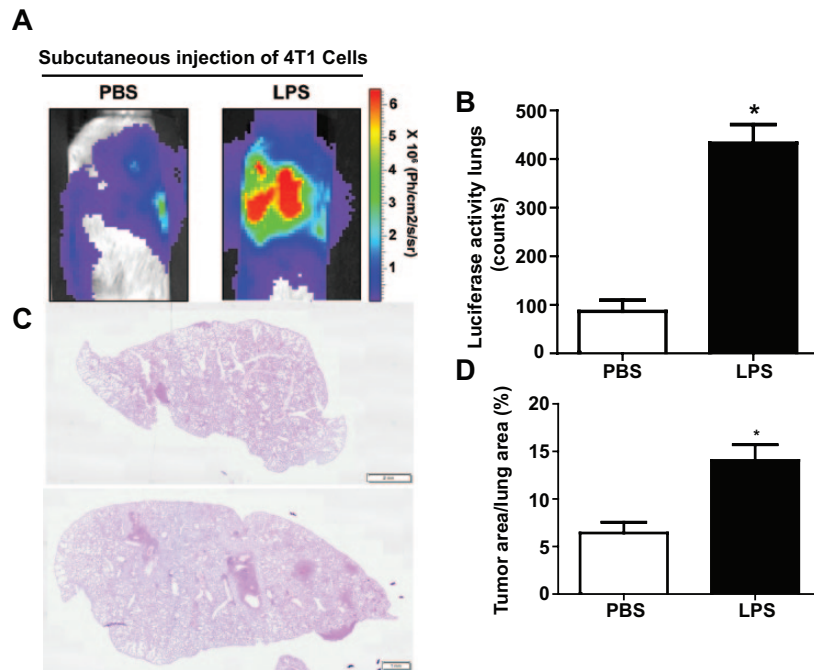
Figure 2. LPS-induced chronic neutrophilic inflammation correlates with lung metastasis. (A) Representative biophotonic monitoring images of lung metastasis in animals subcutaneously injected with 4T1 cells and treated with intratracheal injections of either PBS or LPS. (B) Bioluminescence quantification of tumor foci in lungs by determining regions of interest (ROI) around lungs. (C) Representative hematoxylin-eosin–stained sections of lung tissues of animals intratracheally instilled with PBS or LPS. Scale bar: 1 mm (hematoxylin-eosin). (D) Tumor size was quantified by measuring the ratio between tumor area and total lung tissue area 28 days after subcutaneous cell injection (n = 8). Results are expressed as mean ± SEM. *P < .05. LPS indicates lipopolysaccharide; PBS, phosphate-buffered saline.

PBS + B16F10 group versus 70.15% ± 6.79% and 77.6% ± 1.02% in LPS and LPS + B16F10 group, respectively). Interestingly, lung tissue area occupied by B16F10 cells was significantly higher in LPS-challenged animals as compared with PBS-treated animals (n = 8; *P < .05; Figure 1D and E). To confirm that these effects are not restricted to B16F10 cells, we tested the effects of neutrophils on 4T1 mammary tumor cells. Balb/c mice were instilled with LPS and intravenously injected with luciferase-expressing 4T1 cells. As expected, LPS-treated mice displayed a strong neutrophil recruitment in lungs (n = 8 per group, 1.02% ± 0.34% and 17.42% ± 2.78% in PBS and PBS + 4T1 group versus 43.52% ± 6.3% and 75.7% ± 3.12% in LPS and LPS + 4T1 group, respectively). Bioluminescence corresponding to 4T1 cell luciferase activity in lungs was significantly higher in LPS-treated mice as compared with corresponding control animals (n = 8; *P < .05; Figure 1F and G). Histologic analysis confirmed that areas occupied by metastases in the lungs of LPS-treated mice were increased (n = 8; *P < .05, Figure 1H and I).

Neutrophils recruited in lung microenvironment promote metastasis from distant tumors

To confirm the effects of neutrophils on spontaneous tumor cell dissemination from a primary tumor, a neutrophilic inflammation was induced by LPS instillations in vivo and metastatic spread of subcutaneously injected tumor cells to lung tissues was analyzed. As expected, LPS-exposed mice showed higher BAL neutrophils as compared with control mice (PBS) (n = 8

per group, 1.92% ± 0.67% and 34.52% ± 4.01% in PBS and PBS + 4T1 group versus 60.95% ± 11.65% and 52.46% ± 2.71% in LPS and LPS + 4T1 group, respectively). Although no difference of primary tumor volume was seen between groups (data not shown), tumor cell dissemination to the lung parenchyma was significantly increased in mice exposed to LPS as compared with PBS-treated mice (n = 8; *P < .05; Figure 2A to D). An important step in metastasis formation is the ability of tumor cells to adhere to the endothelium and extravasate from the bloodstream. Therefore, the ability of 4T1 breast cancer cells to extravasate to lung tissues in response to LPS was analyzed in vivo. Interestingly, the number of extravasated 4T1 cells detected in lungs of LPS-exposed mice was significantly higher as compared with control (PBS) groups (n = 6; *P < .05; Figure 3A and B). To determine whether soluble factors directly released from neutrophils promote cancer cell migration, a Boyden chamber assay was used. Interestingly, medium conditioned by LPS-stimulated human neutrophils (neutrophil + LPS SN) enhanced 4T1 and B16F10 cell migration as compared with medium conditioned by nonstimulated neutrophils (neutrophil + PBS SN) (**P < .01; ***P < .001; Figure 3C).

Neutrophils produce increased levels of MMP-9 that generate ac–PGP peptide

Cytokine Antibody Array performed on lung protein extracts from mice bearing subcutaneous tumors identified Pro-MMP-9 as being overexpressed in LPS-treated samples (Supplementary Figure 1). MMP-9, a potential trigger for
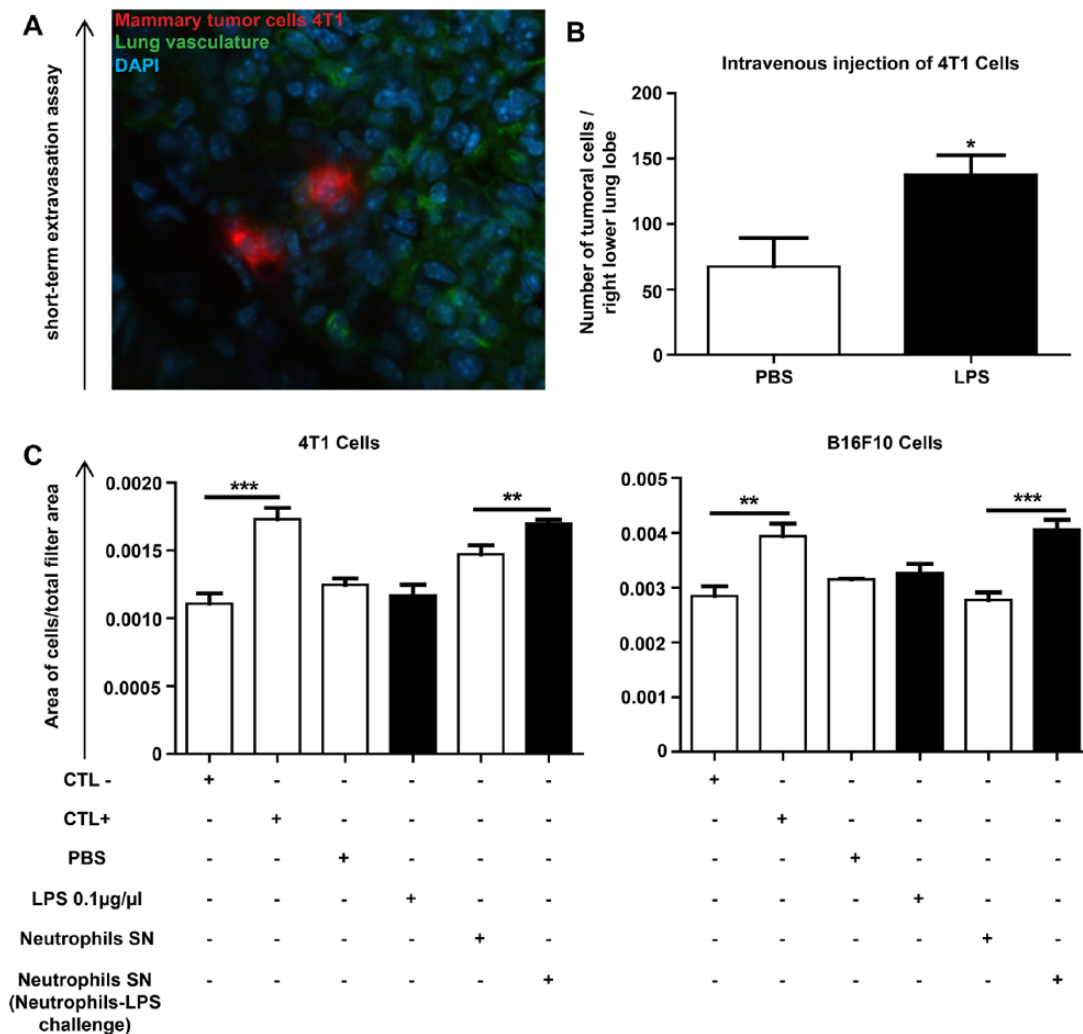
Figure 3. Soluble factors released on neutrophil activation favor tumor cell migration and extravasation. (A) Intravenously injected red-fluorescent 4T1 cells, which extravasated from the FITC-lectin–labeled lung blood vessels (green). Blue staining represents cell nuclei (DAPI) (scale bar: 50 µm). Images were taken 48 hours after tumor cell injection. (B) Quantification of extravasated tumor cells to lungs of mice pretreated with PBS or LPS instillations (n = 6). (C) Quantification of tumor cell chemotaxis (Boyden chamber assay). Tumor cell (4T1 or B16F10 cells) migration was estimated by calculating the ratio between the areas occupied by tumor cells on total filter area from 6 random fields (original magnification 200×). Experiments have been performed in triplicates. Results are expressed as mean ± SEM. *P < .05; **P < .01; ***P < .001. (CTL–: BSA 1%; CTL+: 10% FBS; SN: supernatant). BSA indicates bovine serum albumin; FBS, fetal bovine serum; LPS, lipopolysaccharide; PBS, phosphate-buffered saline.

tumor cell metastasis, was reported to be active on native collagen resulting in the formation of ac-PGP. Interestingly, in this model, serum samples of mice treated with LPS and subcutaneously injected with mammary 4T1 tumor cells displayed detectable levels of ac-PGP (40.5 pg/mL), whereas serum samples derived from PBS-treated animals did not (Figure 4A). To evaluate whether ac-PGP peptides contribute to tumor cell colonization in lungs, mice were treated with intratracheal instillations of synthetic ac-PGP (250 µg/200 µL PBS) or PBS and intravenously injected with 4T1 cells. Interestingly, tumor cell colonization in lungs significantly increased when mice were instilled with ac-PGP (n = 5,*P < .05, ***P < .001, Figure 4B and C). Moreover, instilled ac-PGP peptides were measured in serum samples of ac-PGP–treated mice (58.9 pg/mL), suggesting a possible systemic effect for those fragments (data not shown). To test the specificity of ac-PGP peptide, mice were instilled with a control synthetic tripeptide (ac-VAV

peptide) or PBS and intravenously injected with 4T1 cells. No differences in lung metastasis were observed between experimental groups (n = 5; Figure 4D and E).

Ac–PGP peptide promotes tumor cell recruitment via CXCR2 receptors

CXCR2, a receptor that binds ac-PGP peptides, is present on 4T1 tumor cell surface (data not shown). To evaluate the involvement of ac-PGP-CXCR2 axis in neutrophil-stimulated tumor cell colonization, 4T1 cells transfected with shRNA targeting CXCR2 (4T1-shCXCR2) were intravenously injected in mice previously instilled with either ac-PGP (250 µg/200 µL) or PBS. Animals injected with 4T1-shCXCR2 cells displayed no differences in lung tumor area after ac-PGP treatment (n = 5, Figure 4F and G) as compared with mice injected with 4T1 cells which showed an increase in tumor area/lung area ratio (Figure 4B and C).
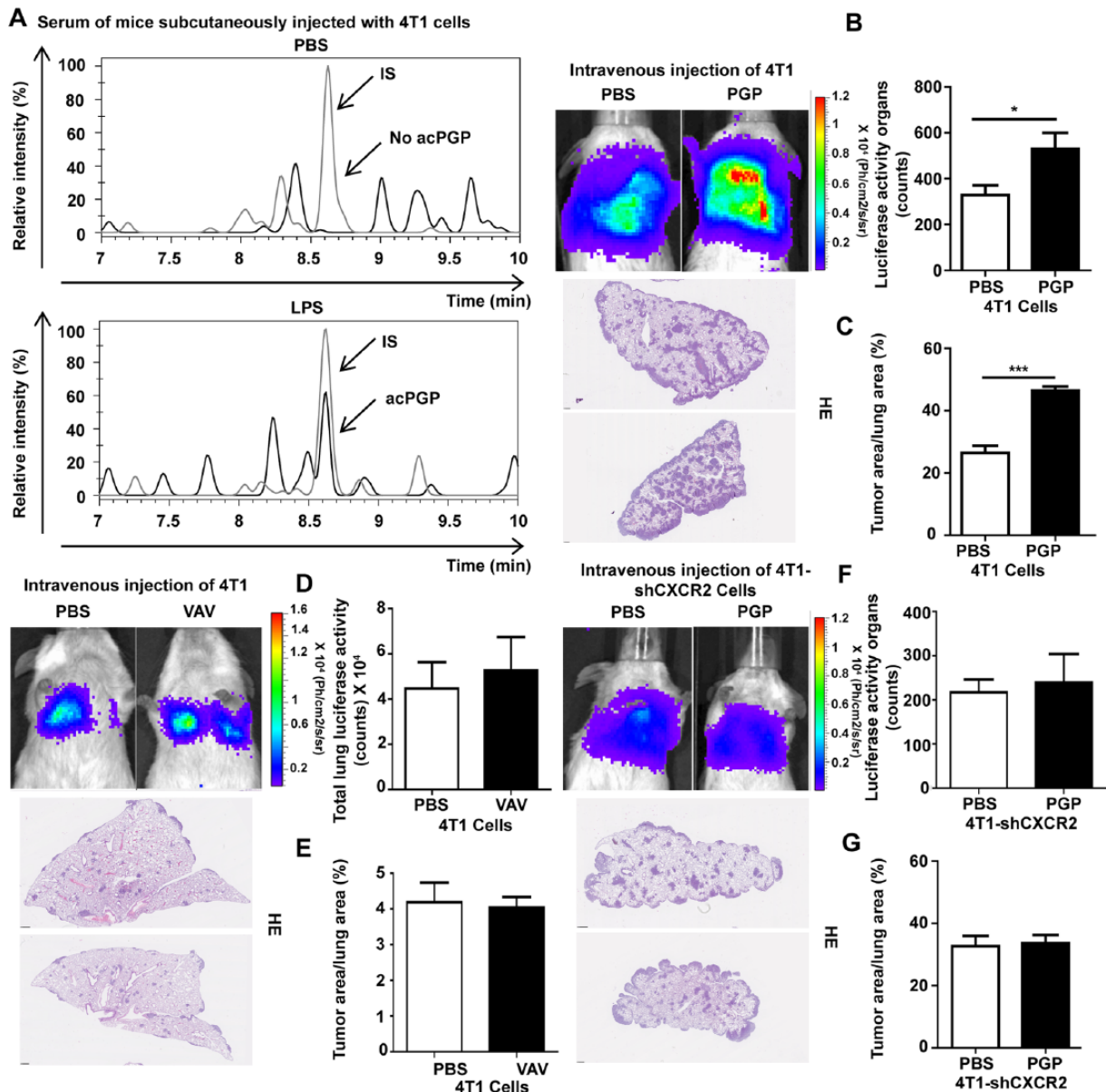
Figure 4. Ac-PGP originating from MMP-9–mediated collagen matrix breakdown induces the recruitment of tumor cells to lung tissues by producing ac-PGP peptides that recruit tumor cells via CXCR2 receptors. (A) Measurement of ac-PGP in serum of mice subcutaneously injected with 4T1 cells and treated with PBS or LPS using LC-MS/MS (representative run). (B, D, F) Bioluminescent monitoring of animals intravenously injected with 4T1 cells or 4T1—shCXCR2 cells and treated with intratracheal instillation of PBS, ac-PGP or ac-VAV (n = 5/group). Bioluminescence quantification of tumors by determining regions of interest (ROI) around lungs. (C, E, G) Representative hematoxylin-eosin–stained sections of lung tissues (hematoxylin-eosin). Scale bar: 1 mm. Tumor size was quantified by measuring the ratio between tumor area and total lung tissue area 14 days after intravenous cell injection. Results are expressed as mean ± SEM. *$P < .05$; ***$P < .001$. Ac-PGP indicates *N*-acetyl-proline-glycine-proline; ac-VAV, *N*-acetyl valine-alanine-valine; LPS, lipopolysaccharide; MMP-9, matrix metalloproteinase 9; PBS, phosphate-buffered saline.

MMP-9 depletion reduces ac–PGP production and lung metastasis

To demonstrate the importance of MMP-9 in ac-PGP release in our model, C57Bl/6 MMP-9$^{+/+}$ and MMP-9$^{-/-}$ mice were intravenously injected with B16F10 and treated with LPS. As expected, lower levels of ac-PGP were observed in serum samples of MMP-9$^{-/-}$ mice treated with LPS (121 pg/mL) as compared with MMP-9$^{+/+}$ mice (194 pg/mL) (Figure 5A). Histologic quantification of lung metastasis showed a significant increase in lung tumor area in LPS-treated MMP-9$^{+/+}$

and MMP-9$^{-/-}$ mice. However, area occupied by lung metastasis in LPS-treated MMP-9$^{-/-}$ was significantly lower than in MMP-9$^{+/+}$, suggesting an implication of MMP-9 in the neutrophil-driven metastatic dissemination of tumor cells via ac-PGP peptides (n = 6, *$P < .05$; Figure 5B and C).

Discussion

Understanding molecular mechanisms governing metastatic dissemination is a key issue for the development of cancer therapies. In this study, our main purpose was to decipher the
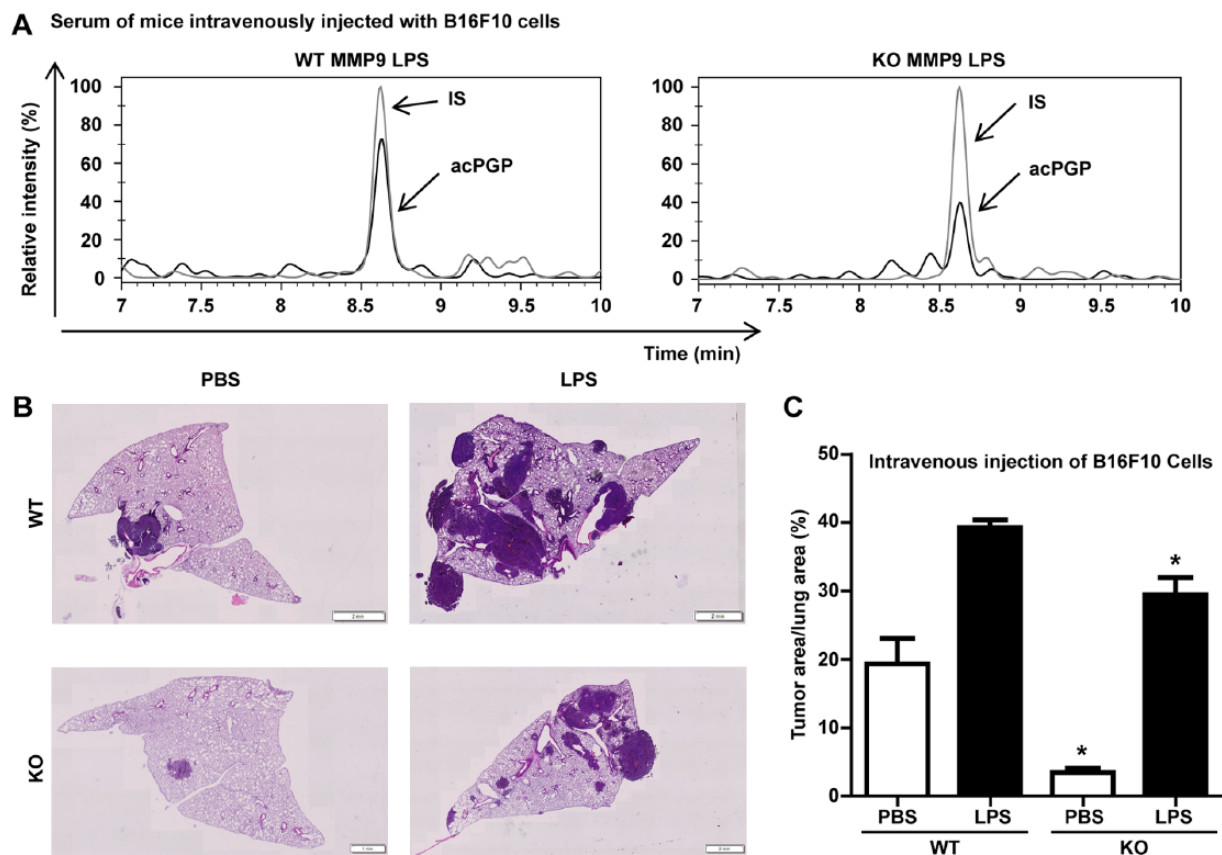
Figure 5. MMP-9 participates in the ac-PGP release in lungs. (A) Measurement of ac-PGP in serum of MMP-9^{+/+} and MMP-9^{−/−} mice intravenously injected with B16F10 cells and treated with LPS using LC-MS/MS (representative run). (B) Representative hematoxylin-eosin–stained lung sections of MMP-9^{+/+} and MMP-9^{−/−} mice 2 weeks after intravenous B16F10 melanoma injection (hematoxylin-eosin). Scale bar: 1 mm. (C) Tumor size was quantified by measuring the ratio between area occupied by tumor foci and total lung tissue area on hematoxylin-eosin–stained tissue sections (n = 6/group; hematoxylin-eosin). Results are expressed as mean ± SEM. *$P < .05$. Ac-PGP indicates *N*-acetyl-proline-glycine-proline; LPS, lipopolysaccharide; MMP-9, matrix metalloproteinase 9.

impact on lung metastasis of extracellular matrix fragments generated in the context of inflammation. We report that neutrophil accumulation generated by CS and LPS facilitates the implantation of metastatic cells into lung tissues in an MMP-9-ac-PGP-CXCR2–dependent manner. This paradigm is supported by (1) the measurement of increased tumor cell dissemination to lungs following the induction of a pulmonary neutrophilic inflammation, (2) the measurement of increased levels of ac-PGP tripeptides in the serum of LPS-treated animals and subcutaneously injected with tumor cells, (3) the demonstration of an MMP-9–dependent collagen breakdown into chemotactic ac-PGP, (4) enhanced tumor cell colonization to lung tissues after pulmonary ac-PGP treatment, and (5) the inhibition of the effects of ac-PGP on tumor cells accumulation in lungs once CXCR2 is knocked down in tumor cells (Figure 6).

Epidemiologic studies and clinical observations have established links between inflammation, carcinogenesis, and metastasis processes. However, mechanisms linking chronic inflammation to increased tumor development and metastasis remain enigmatic. Recent studies support that 25% of all human cancers result from chronic inflammation.[27–31] Chronic inflammation includes microbial infections,[32] autoimmune diseases,[33] or pollution-driven inflammation. Tobacco smoke appears as a very common pollutant composed of no less than 4700 compounds, comprising many oxidants and influencing cell proliferation, angiogenesis, tumor growth, and metastasis.[34] Nicotine is one major bioactive component of CS displaying a carcinogenic potential by directly inducing cell proliferation and angiogenesis and by protecting cancer cells from apoptosis.[35] We therefore evaluated direct effects of CS on cell proliferation in vivo. We report that CS per se does not enhance tumor cell proliferation in our experimental setting. Although previous authors suggested that tobacco smoke compounds could positively interfere with tumor progression,[36] others have shown a cytotoxic effect of CS due to, eg, *N*-nitrosamines and free radicals.[37] Because it becomes more and more evident that inflammation plays significant roles in metastatic dissemination,[27] we focused our research on inflammation-related changes in lung microenvironment. In our experiments, mice challenged with CS displayed increased lung metastases, which could be facilitated by the neutrophilic inflammation caused by
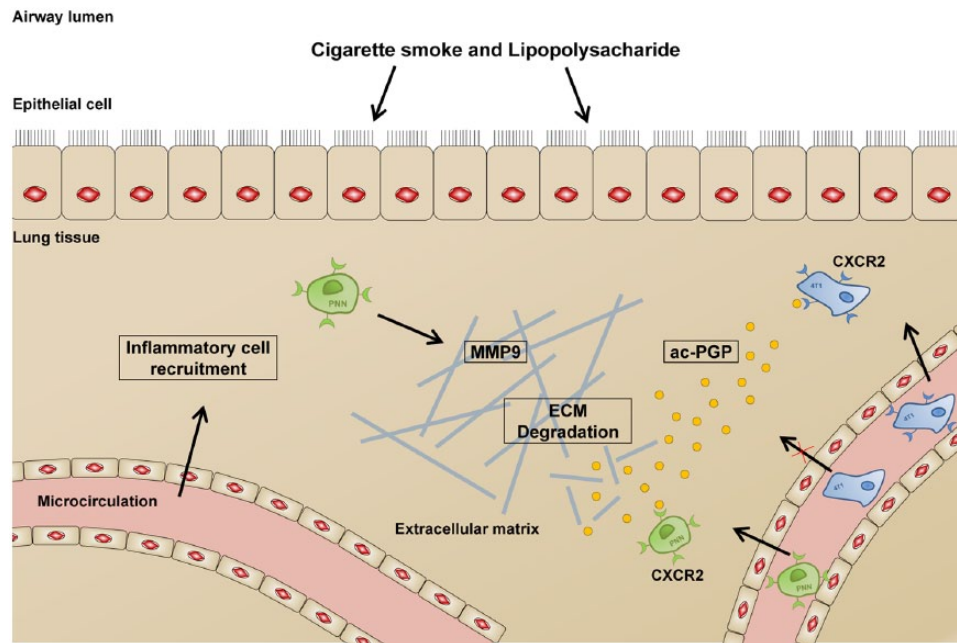
Figure 6. Proposed mechanisms for tumor cell progression in the context of neutrophilic inflammation in the lung. Ac-PGP indicates *N*-acetyl-proline-glycine-proline; ECM, extracellular matrix; MMP-9, matrix metalloproteinase 9.

CS exposure.[9,38,39] To confirm that the metastasis-supporting effect from CS is mostly due to the neutrophilic inflammation, LPS was used to reproduce a similar inflammatory burden. To better reproduce the complex multistep process of tumor metastasis, two different mouse models were applied: (1) a subcutaneous tumor model, where subcutaneously implanted cancer cells undergo all steps of metastasis (intravasation, circulation in bloodstream, extravasation) and (2) a model where tumor cells are intravenously injected and mimic final steps of metastatic dissemination (circulation in bloodstream, extravasation). Two cell lines from different origins were used: mammary tumor cells 4T1 and melanoma cells B16F10. We used these syngeneic models in 2 genetic backgrounds in immunocompetent mice (BALB/c and C57/bl6) to avoid any putative influence of immune deficiency in mice. The increase in lung metastases in mice treated with LPS provides evidence for a central role of neutrophils in metastatic dissemination. Furthermore, we show that ex vivo LPS-induced neutrophil activation stimulates tumor cell migration in vitro, suggesting a direct role of neutrophils in cancer cell migration by releasing chemoattractant proteins or other protumor or prometastasis molecules, such as matrix metallopeptidases including MMP-9. Indeed, previous studies have shown that MMP-9 is stored in specific granules from neutrophils and is found in sputum of patients with asthma and COPD.[15,40] Moreover, MMP-9 could contribute to the establishment of a premetastatic niche and facilitate tumor progression.[41] MMP-9 plays several roles in inflammation, notably through the degradation of extracellular matrix components resulting in the generation of products that include ac-PGP that contribute to inflammatory cell recruitment.[14,42] The relationship between MMP-9 and ac-PGP is demonstrated in this study as ac-PGP levels are decreased in MMP-9$^{-/-}$ mice as compared with MMP-9$^{+/+}$ animals. Ac-PGP instillations increased lung metastasis of intravenously injected cancer cells, which confirms the direct implication of ac-PGP in the metastatic cascade. The matrikin ac-PGP has been described by Weathington et al[24] and other authors to recruit neutrophils to the lung parenchyma in a CXCR2-dependent mechanism.[12,13] We demonstrate here the key role of ac-PGP and CXCR2 in lung metastases burden following lung inflammation. Altogether, we establish with these experiments a link between pulmonary neutrophilic inflammation, ac-PGP peptides, MMP-9, CXCR2 surface receptor, and increased metastatic dissemination.

Many therapeutic perspectives could derive from these data as ac-PGP or CXCR2 blockade might represent attractive therapeutic targets to decrease lung metastasis in patients with established primary tumors or in a preventive manner in high-risk patients. Some therapeutic options already exist for patients with COPD to decrease ac-PGP levels using azithromycin,[43] and valproic acid is able to reduce the production of ac-PGP by inhibiting the downstream cleavage of collagen-derived peptides by prolyl endopeptidase.[44] Another promising therapeutic perspective would be to enhance the ac-PGP clearance by a restoration of the leukotriene A4 aminopeptidase activity through a dedicated pharmacologic agent.[45] Other studies will be needed to confirm our findings and establish the validity of such a therapeutic strategy in patients with cancer.

In conclusion, our data demonstrate that pulmonary accumulation of neutrophils increases lung metastasis of tumor cells in an MMP-9–dependent manner by the production of collagen-derived ac-PGP chemotactic peptides that engage CXCR2 present at the surface of cancer cells.

Acknowledgements

Author Contributions

Availability of data and material

Data sharing is not applicable to this article as no data sets were generated or analyzed during this study.

Ethical Approval and Consent to Participate

Ethical Committee of the University of Liège approved the protocols used for animal studies under the references #736, #918, #1667. There were no clinical samples in this study.

REFERENCES

1. Gupta GP, Massague J. Cancer metastasis: building a framework. *Cell.* 2006;127:679–695.
2. Fridlender ZG, Sun J, Kim S, et al. Polarization of tumor-associated neutrophil phenotype by TGF-beta: "N1" versus "N2" TAN. *Cancer Cell.* 2009;16: 183–194.
3. Sica A, Mantovani A. Macrophage plasticity and polarization: in vivo veritas. *J Clin Invest.* 2012;122:787–795.
4. Balkwill F, Charles KA, Mantovani A. Smoldering and polarized inflammation in the initiation and promotion of malignant disease. *Cancer Cell.* 2005;7: 211–217.
5. Young RP, Hopkins RJ, Christmas T, Black PN, Metcalf P, Gamble GD. COPD prevalence is increased in lung cancer, independent of age, sex and smoking history. *Eur Respir J.* 2009;34:380–386.
6. Shaul ME, Fridlender ZG. Neutrophils as active regulators of the immune system in the tumor microenvironment. *J Leukoc Biol.* 2017;102:343–349.
7. Powell HA, Iyen-Omofoman B, Baldwin DR, Hubbard RB, Tata LJ. Chronic obstructive pulmonary disease and risk of lung cancer: the importance of smoking and timing of diagnosis. *J Thorac Oncol.* 2013;8:e34–e35.
8. Blidberg K, Palmberg L, Dahlen B, Lantz AS, Larsson K. Increased neutrophil migration in smokers with or without chronic obstructive pulmonary disease. *Respirology.* 2012;17:854–860.
9. Blidberg K, Palmberg L, Dahlen B, Lantz AS, Larsson K. Chemokine release by neutrophils in chronic obstructive pulmonary disease. *Innate Immun.* 2012;18:503–510.
10. Granot Z, Fridlender ZG. Plasticity beyond cancer cells and the "immunosuppressive switch." *Cancer Res.* 2015;75:4441–4445.
11. Wculek SK, Malanchi I. Neutrophils support lung colonization of metastasis-initiating breast cancer cells. *Nature.* 2015;528:413–417.
12. Overbeek SA, Kleinjan M, Henricks PA, et al. Chemo-attractant N-acetyl proline-glycine-proline induces CD11b/CD18-dependent neutrophil adhesion. *Biochim Biophys Acta.* 2013;1830:2188–2193.
13. Xu X, Jackson PL, Tanner S, et al. A self-propagating matrix metalloprotease-9 (MMP-9) dependent cycle of chronic neutrophilic inflammation. *PLoS ONE.* 2011;6:e15781.
14. Gaggar A, Jackson PL, Noerager BD, et al. A novel proteolytic cascade generates an extracellular matrix-derived chemoattractant in chronic neutrophilic inflammation. *J Immunol.* 2008;180:5662–5669.
15. Cataldo D, Munaut C, Noel A, et al. Matrix metalloproteinases and TIMP-1 production by peripheral blood granulocytes from COPD patients and asthmatics. *Allergy.* 2001;56:145–151.
16. Braber S, Koelink PJ, Henricks PA, et al. Cigarette smoke-induced lung emphysema in mice is associated with prolyl endopeptidase, an enzyme involved in collagen breakdown. *Am J Physiol Lung Cell Mol Physiol.* 2011;300: L255–L265.
17. Pfister RR, Haddox JL, Sommers CI. Injection of chemoattractants into normal cornea: a model of inflammation after alkali injury. *Invest Ophthalmol Vis Sci.* 1998;39:1744–1750.
18. Pfister RR, Haddox JL, Sommers CI, Lam KW. Identification and synthesis of chemotactic tripeptides from alkali-degraded whole cornea. A study of N-acetyl-proline-glycine-proline and N-methyl-proline-glycine-proline. *Invest Ophthalmol Vis Sci.* 1995;36:1306–1316.
19. Kim SD, Lee HY, Shim JW, et al. Activation of CXCR2 by extracellular matrix degradation product acetylated Pro-Gly-Pro has therapeutic effects against sepsis. *Am J Respir Crit Care Med.* 2011;184:243–251.
20. Keane MP, Burdick MD, Xue YY, Lutz M, Belperio JA, Strieter RM. The chemokine receptor, CXCR2, mediates the tumorigenic effects of ELR+ CXC chemokines. *Chest.* 2004;125:133S.
21. Saintigny P, Massarelli E, Lin S, et al. CXCR2 expression in tumor cells is a poor prognostic factor and promotes invasion and metastasis in lung adenocarcinoma. *Cancer Res.* 2013;73:571–582.
22. Nannuru KC, Sharma B, Varney ML, Singh RK. Role of chemokine receptor CXCR2 expression in mammary tumor growth, angiogenesis and metastasis. *J Carcinog.* 2011;10:40.
23. O'Reilly P, Jackson PL, Noerager B, et al. N-alpha-PGP and PGP, potential biomarkers and therapeutic targets for COPD. *Respir Res.* 2009;10:38.
24. Weathington NM, van Houwelingen AH, Noerager BD, et al. A novel peptide CXCR ligand derived from extracellular matrix degradation during airway inflammation. *Nat Med.* 2006;12:317–323.
25. Vu TH, Shipley JM, Bergers G, et al. MMP-9/gelatinase B is a key regulator of growth plate angiogenesis and apoptosis of hypertrophic chondrocytes. *Cell.* 1998;93:411–422.
26. Marée R, Stevens B, Louppe G, et al. A hybrid human-computer approach for largescale image-based measurements using web services and machine learning. Paper presented at: Proceedings IEEE International Symposium on Biomedical Imaging; 29 April-2 May, 2014; Beijing, China.
27. Balkwill F, Mantovani A. Inflammation and cancer: back to Virchow? *Lancet.* 2001;357:539–545.
28. Coussens LM, Werb Z. Inflammation and cancer. *Nature.* 2002;420:860–867.
29. Hussain SP, Harris CC. Inflammation and cancer: an ancient link with novel potentials. *Int J Cancer.* 2007;121:2373–2380.
30. Mantovani A, Allavena P, Sica A, Balkwill F. Cancer-related inflammation. *Nature.* 2008;454:436–444.
31. Houghton AM. Mechanistic links between COPD and lung cancer. *Nat Rev Cancer.* 2013;13:233–245.
32. Collins D, Hogan AM, Winter DC. Microbial and viral pathogens in colorectal cancer. *Lancet Oncol.* 2011;12:504–512.
33. Das Roy L, Pathangey LB, Tinder TL, Schettini JL, Gruber HE, Mukherjee P. Breast-cancer-associated metastasis is significantly increased in a model of autoimmune arthritis. *Breast Cancer Res.* 2009;11:R56.
34. Davis R, Rizwani W, Banerjee S, et al. Nicotine promotes tumor growth and metastasis in mouse models of lung cancer. *PLoS ONE.* 2009;4:e7524.
35. Martinez-Garcia E, Irigoyen M, Gonzalez-Moreno O, et al. Repetitive nicotine exposure leads to a more malignant and metastasis-prone phenotype of SCLC: a molecular insight into the importance of quitting smoking during treatment. *Toxicol Sci.* 2010;116:467–476.
36. Nakada T, Kiyotani K, Iwano S, et al. Lung tumorigenesis promoted by anti-apoptotic effects of cotinine, a nicotine metabolite through activation of PI3K/Akt pathway. *J Toxicol Sci.* 2012;37:555–563.
37. Kode A, Yang SR, Rahman I. Differential effects of cigarette smoke on oxidative stress and proinflammatory cytokine release in primary human airway epithelial cells and in a variety of transformed alveolar epithelial cells. *Respir Res.* 2006;7:132.
38. Joyce JA, Pollard JW. Microenvironmental regulation of metastasis. *Nat Rev Cancer.* 2009;9:239–252.
39. Wu Y, Zhou BP. Inflammation: a driving force speeds cancer metastasis. *Cell Cycle.* 2009;8:3267–3273.

40. Van den Steen PE, Proost P, Wuyts A, Van Damme J, Opdenakker G. Neutrophil gelatinase B potentiates interleukin-8 tenfold by aminoterminal processing, whereas it degrades CTAP-III, PF-4, and GRO-alpha and leaves RANTES and MCP-2 intact. *Blood*. 2000;96:2673–2681.

41. Deryugina EI, Quigley JP. Pleiotropic roles of matrix metalloproteinases in tumor angiogenesis: contrasting, overlapping and compensatory functions. *Biochim Biophys Acta*. 2010;1803:103–120.

42. O'Reilly PJ, Hardison MT, Jackson PL, et al. Neutrophils contain prolyl endopeptidase and generate the chemotactic peptide, PGP, from collagen. *J Neuroimmunol*. 2009;217:51–54.

43. O'Reilly PJ, Jackson PL, Wells JM, Dransfield MT, Scanlon PD, Blalock JE. Sputum PGP is reduced by azithromycin treatment in patients with COPD and correlates with exacerbations. *BMJ Open*. 2013;3: e004140.

44. Roda MA, Sadik M, Gaggar A, et al. Targeting prolyl endopeptidase with valproic acid as a potential modulator of neutrophilic inflammation. *PLoS ONE*. 2014;9:e97594.

45. Paige M, Wang K, Burdick M, et al. Role of leukotriene A4 hydrolase aminopeptidase in the pathogenesis of emphysema. *J Immunol*. 2014;192: 5059–5068.